Aluminum-Decorated MIL-100(Fe) Nanozyme for the Detection of Glutathione

Lin Cui,[⊥] Xinshuo Zhao,[⊥] Jiankang Zhang,[*,⊥] Zhan Zhou, Dong Lin, and Yong Qin

ACCESS | Metrics & More | Article Recommendations | Supporting Information

ABSTRACT: Nanozymes are nanomaterials with natural enzyme characteristics, which are expected to be potential substitutes of traditional enzymes. In this study, the 1Al/MIL-100(Fe) nanozymes with excellent peroxidase-like activity were synthesized by the ultrathin modification (one-cycle Al_2O_3) strategy of atomic layer deposition, whose peroxidase-like activity is almost doubled compared with MIL-100(Fe) nanozymes. Investigation of the catalytic mechanism indicates that the increased amount of hydroxyl radical is responsible for the much-enhanced peroxidase-like activity of 1Al/MIL-100(Fe) nanozymes. Furthermore, the catalytic effect of the designed nanozymes is inhibited by glutathione through consuming the oxidized 3,3′,5,5′-tetramethylbenzidine in the reaction system. The 1Al/MIL-100(Fe) nanozymes also achieve the sensitive and selective detection of glutathione, which have an excellent linear response to glutathione concentration in the range 0.01−1000 μM with a detection limit of 2.2 nM. The ultrathin modification strategy can be potentially extended to synthesize other high-efficiency nanozyme materials.

KEYWORDS: *nanozymes, atomic layer deposition, ultrathin modification, peroxidase-like activity, glutathione*

1. INTRODUCTION

Nanozyme is a new generation of artificial enzyme, which has the advantages of adjustable catalytic activity, low cost of ownership, and good stability.[1−16] Due to their extensive potential applications, nanozymes have emerged as a burgeoning field that bridges biology and nanotechnology.[17−32] However, the activity and selectivity of nanozymes still need to be improved, and the biocompatibility is also a challenging issue.[2] In order to overcome the above constraints, various strategies have been suggested to control the catalytic activity of nanozymes by means of surface modification, element doping, or construction of composite nanomaterials,[18] among which surface modification has been an effective strategy to improve the nanozyme performance.

Atomic layer deposition (ALD) is an advanced tool for the precise preparation of specifically structured nanomaterials, which can achieve fine control of the structures of nanomaterials at the atomic level.[33−39] ALD has been widely used in the traditional catalysis field, and especially the ultrathin modification strategy was used to synthesize catalysts with a specific structure. However, the synthesis of high-efficiency nanozymes by using the ultrathin modification strategy of ALD has been rarely reported in the nanozyme field.

In this work, the atomically dispersed nanozyme named 1Al/MIL-100(Fe) was synthesized based on the Al_2O_3 ALD process (one-cycle Al_2O_3 ultrathin modification toward MIL-100(Fe)), which can simulate the activity of peroxidase by decomposing H_2O_2 into the hydroxyl radical (·OH), and present much-enhanced peroxidase activity compared with the as-prepared counterparts in the characteristic colorimetric hydrogen peroxide (H_2O_2)−3,3′,5,5′-tetramethylbenzidine (TMB) reaction. By utilizing this characteristic, 1Al/MIL-100(Fe) nanozymes also show great potential in developing

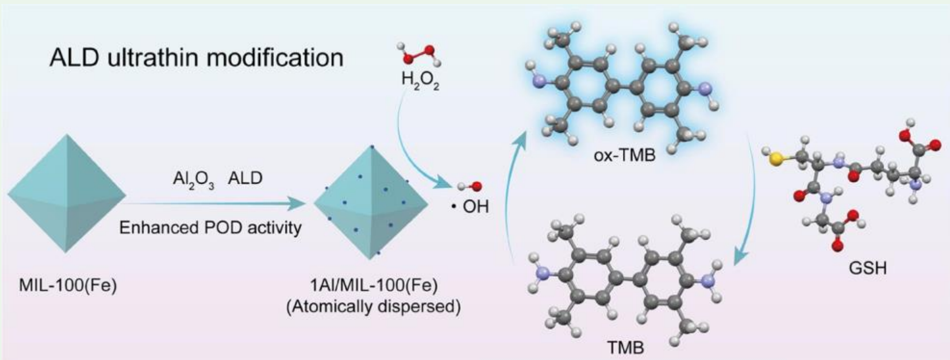

ALD ultrathin modification
H_2O_2
Al_2O_3 ALD
Enhanced POD activity
• OH
ox-TMB
GSH
MIL-100(Fe)
1Al/MIL-100(Fe)
(Atomically dispersed)
TMB

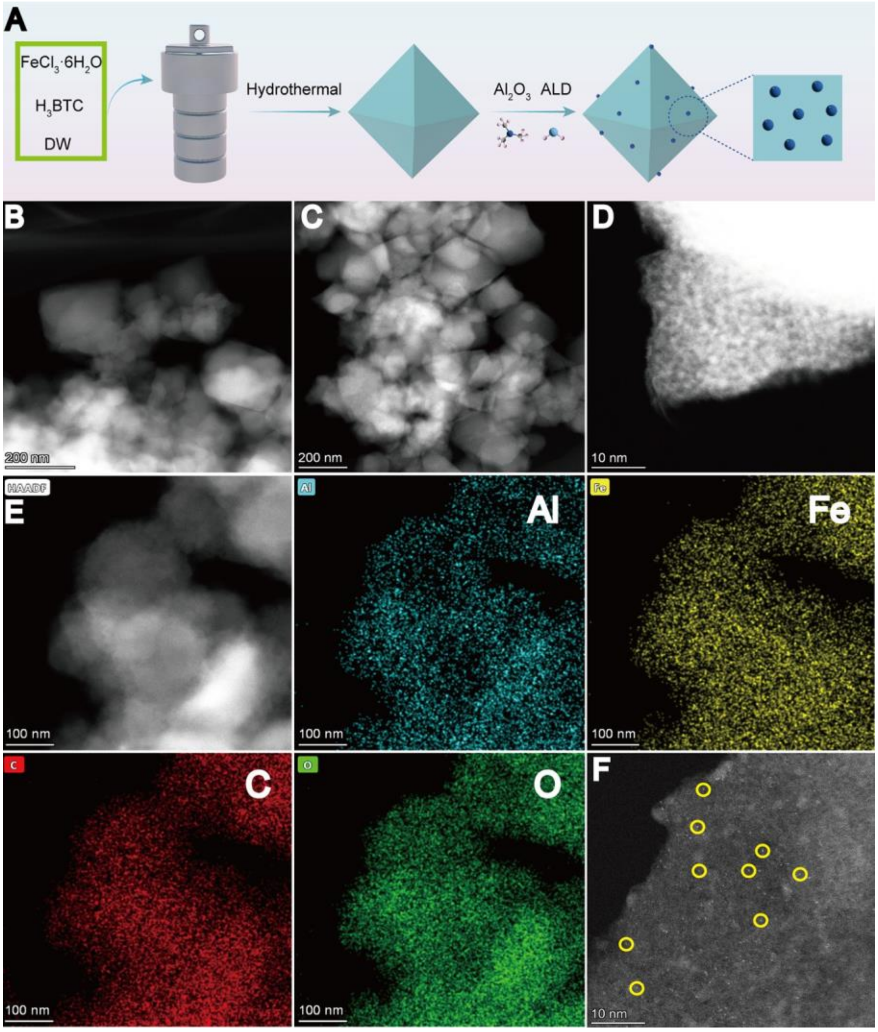

Figure 1. (A) Synthetic process of 1Al/MIL-100(Fe) by the ultrathin modification strategy. (B) HAADF-STEM images of the MIL-100(Fe) nanozymes. (C−E) HAADF-STEM images of 1Al/MIL-100(Fe) and the EDS mapping images of Al, Fe, C, and O. (F) HAADF-STEM images of 1Al/C (the white dots are Al single atoms, and parts of them are labeled by the yellow circles). DW represents deionized water.

high-efficiency sensitive biosensors. A colorimetric strategy based on 1Al/MIL-100(Fe) nanozymes has also been developed for the quantitative detection of glutathione (GSH).

2. EXPERIMENTAL SECTION

2.1. Materials. Sulfoxide (DMSO), hydrogen peroxide (H_2O_2), ethanol (C_2H_6O), isopropyl alcohol (IPA), sodium acetate trihydrate ($CH_3COONa{\cdot}3H_2O$), acetic acid (CH_3COOH), iron(III) chloride hexahydrate ($FeCl_3{\cdot}6H_2O$), trimesic acid (H_3BTC), sodium chloride (NaCl), calcium chloride ($CaCl_2$), and potassium chloride (KCl) were obtained from Shanghai Sinopharm Chemical Reagent Co., Ltd. Glutathione (GSH), 3,3′,5,5′-tetramethylbenzidine (TMB), cysteine (Cys), threonine (Thr), lysine (Lys), glycine (Gly), histidine (His), and arginine (Arg) were purchased from Shanghai Aladdin Chemical Co., Ltd. Terephthalic acid (TA) was acquired from Shanghai Macklin Biochemical Technology Co. Trimethylaluminum (Alfa Aesar, 25 wt % in hexane) and titanium tetraisopropoxide (Alfa Aesar, 97%) were obtained from J&K Scientific. Ultrapure water was used for all the experiments.

2.2. Nanozyme Characterizations. Transmission electron microscopy (TEM), high-angle annular dark-field scanning TEM and energy-dispersive X-ray spectroscopy mapping images were obtained by operating a transmission electron microscope (Themis FEI) at 300 kV. Scanning electron microscopy (SEM) images were acquired by a scanning electron microscope (ZEISS Sigma 500, USA). X-ray diffraction (XRD) patterns were obtained by using Cu Kα radiation. N_2 adsorption−desorption experiments were performed by Beishide Instrument Technology (Beijing) Co., Ltd. (BSD-PS(M)). X-ray photoelectron spectroscopy (XPS) was performed by using the Al-Ka line as the radiation source. The generation of ·OH was measured by an electron spin resonance (ESR) spectrometer (Bruker ESR A300), with DMPO as the spin trap.

2.3. Ultrathin Modification of MIL-100(Fe) Nanozymes. The MIL-100(Fe) carrier was first obtained by a slight adjustment based on the previously reported method. Briefly, $FeCl_3{\cdot}6H_2O$ (5.4 g) and H_3BTC (3.78 g) were placed in 12 mL of ultrapure water and dissolved uniformly by ultrasonication. The prepared solution was then transferred to 25 mL of the reactor and maintained at 95 °C for 18 h. After the completion of the reaction, the precipitate was separated through centrifugation and three washes with 50% (v/v) ethanol/water to obtain the MIL-100(Fe) carrier. Eventually, the MIL-100(Fe) solid powder was prepared by vacuum-drying overnight.[40,41] Then, the ultrathin-modified *x*Al/MIL-100(Fe) nanozymes (x represents the number of Al_2O_3 ALD cycles) were obtained by conducting an Al_2O_3 ALD process with C_3H_9Al and deionized H_2O as the precursor and oxidant, respectively. The deposition temperature was set at 130 °C. The pulse, exposure, and purge times for C_3H_9Al and H_2O were 0.02/8/32 and 0.1/9/32 s, respectively. By adjusting the number of cycles in this procedure, several *x*Al/MIL-100(Fe) nanozymes were prepared (x = 0, 1, 3, 6, 12).

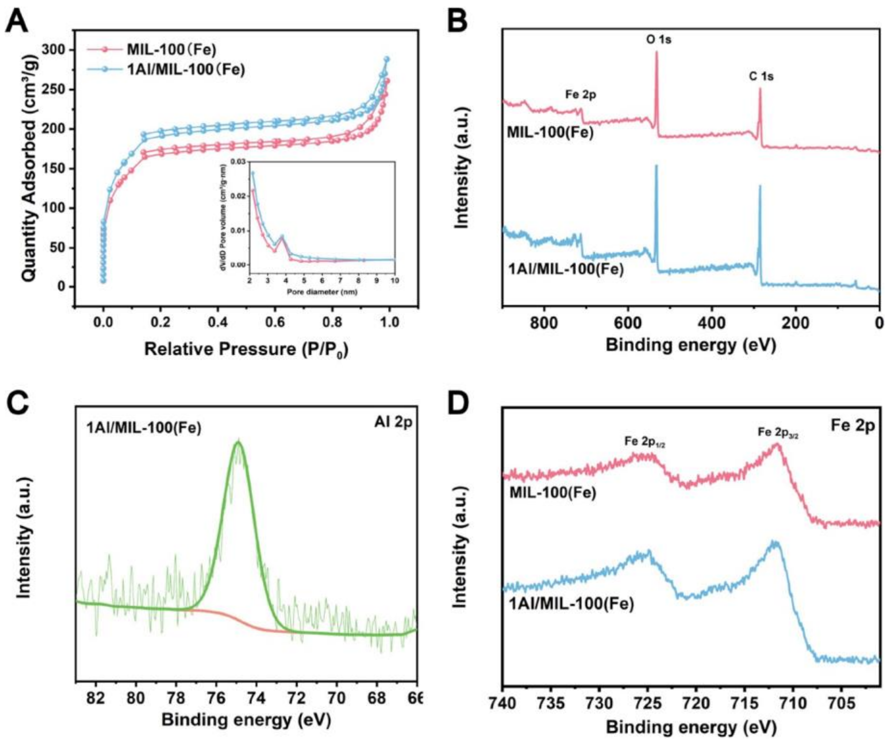

Figure 2. (A) N_2 sorption isotherms and pore size distribution (inset) of the two nanozymes. (B) XPS survey spectra of the two nanozymes. (C) XPS Al 2p spectrum of 1Al/MIL-100(Fe). (D) Fe 2p spectra of the two nanozymes.

2.4. Evaluation of Peroxidase-Like Activity. The peroxidase-like activity of the nanozymes was evaluated by using a typical chromogenic reaction with H_2O_2 and TMB as substrates. The HAc−NaAc buffer solution (pH = 3.6, 0.2 M) including TMB (0.5 mM), H_2O_2 (1 mM), and 1Al/MIL-100(Fe) (0.04 mg mL^{-1}) was mixed and incubated for 10 min at 37 °C. The colorless TMB can be oxidized to oxidized TMB (ox-TMB, $\varepsilon_{652\ nm}$ = 39,000 M^{-1} cm^{-1}). The reaction absorbance was measured using an ultraviolet−visible spectrophotometer to record the peroxidase-like activity.

2.5. Colorimetric Detection of Glutathione. Colorimetric detection of glutathione experiment catalyzed by the optimized 1Al/MIL-100(Fe) nanozymes was carried out as follows: GSH with different concentrations was added to HAc−NaAc buffer (pH = 3.6), and then 20 μL of 1Al/MIL-100(Fe) and 100 μL of H_2O_2−TMB substrates were mixed and incubated for 10 min. The mixed solutions were measured using a UV−vis spectrophotometer, and the absorbance at 652 nm was recorded, which is related to the GSH concentration for the quantitative detection of GSH. The detection limit is obtained by the standard formula (LOD = $3\sigma/S$), in which σ and S represent the standard deviation of blank control and slope of the calibration graph, respectively.

3. RESULTS AND DISCUSSION

3.1. Synthesis and Characterization of Nanozymes. Nanozymes (1Al/MIL-100(Fe)) were prepared by the ultrathin modification strategy of ALD, as shown in Figure 1A. In detail, the MIL-100(Fe) supports were first prepared through the hydrothermal synthesis approach; then, Al_2O_3 ALD was conducted to obtain the ultrathin modified xAl/MIL-100(Fe) nanozymes, in which x represents the number of cycles of Al_2O_3 ALD (x = 0, 1, 3, 6, 12). Figure 1B is the HAADF-STEM image of MIL-100(Fe) nanozymes, which present particle morphology (Figure S1A). No obvious change is observed after the decoration of one cycle of Al_2O_3 (Figures 1C and S1B). From the high-resolution TEM image (Figure 1D), no aluminum species is detected owing to the high dispersion, low content (0.07 wt %, ICP-OES), and small difference of Z contrast. However, aluminum, iron, carbon, and oxygen elements can be detected from the EDS mapping images of 1Al/MIL-100(Fe) nanozymes (Figure 1E), indicating the successful deposition of Al_2O_3 on MIL-100(Fe) nanozymes. The ultralow amount of Al on the 1Al/MIL-100(Fe) nanozymes also indicates the potential atomic dispersion of Al on the support. To confirm this speculation, one cycle of Al_2O_3 was deposited on the carbon support. As expected, atomically dispersed Al atoms can be clearly observed (Figure 1F). These results indicate that the 1Al/MIL-100(Fe) nanozymes possess the atomic dispersion property for the ALD-decorated aluminum species.

The physicochemical properties of the nanozymes were further characterized by multiple characterization techniques. To study the textural properties of the nanozymes, N_2 sorption characterization was carried out (Figure 2A). The curves of two samples present properties of mesoporous materials. The specific surface area of the 1Al/MIL-100(Fe) nanozyme increases slightly in comparison to the as-prepared counterparts, while the pore size distribution is nearly unchanged (Table S1). To investigate the microstructure of MIL-100(Fe) and 1Al/MIL-100(Fe) nanozymes, XRD was performed (Figure S2). It can be seen that the peaks of MIL-100(Fe) and 1Al/MIL-100(Fe) are quite similar, which suggests that the ALD process exerts little influence on the structure of MIL-100(Fe). No peak ascribed to aluminum species is detected owing to the high dispersion and low content. The electronic property of the elements was characterized by XPS, according to Figure 2B−D. From the fine Al 2p spectrum of 1Al/MIL-100(Fe) nanozymes (Figure 2C), the peak at around 74.9 eV ascribed to Al 2p can be observed, and this again indicates the successful modification of Al_2O_3 on MIL-100(Fe) nanozymes. For the XPS Fe 2p spectra of MIL-100(Fe) nanozymes and

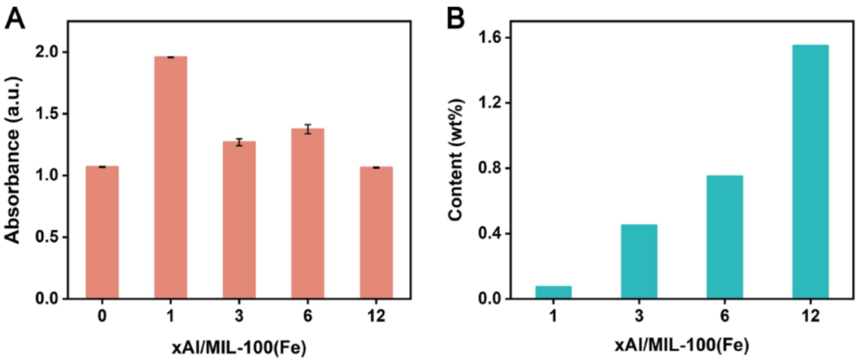

Figure 3. (A) Comparison of peroxidase-like activity catalyzed by *x*Al/MIL-100(Fe) nanozymes. (B) Al content of *x*Al/MIL-100(Fe) nanozymes.

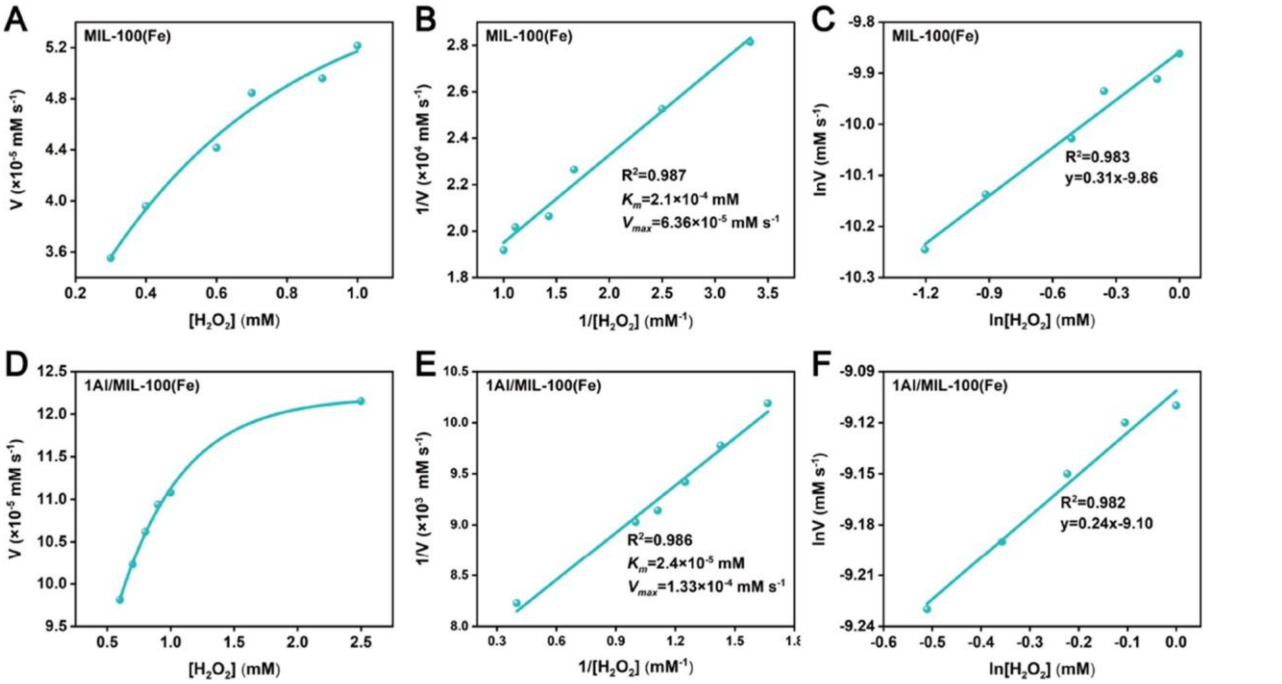

Figure 4. (A, D) Initial reaction rate as a function of [H_2O_2] for 10 min of incubation over the two nanozymes. (B, E) Lineweaver−Burk plots of 1/V vs 1/[H_2O_2] over the two nanozymes. (C, F) Plots of ln *V* against ln[H_2O_2] over the two nanozymes.

1Al/MIL-100(Fe) nanozymes (Figure 2D), no obvious shift is observed, indicating that the electronic state of Fe is almost unchanged before and after the ultrathin modification of aluminum species.

3.2. Peroxidase-Like Activity Evaluation and Steady-State Kinetic Studies of Nanozymes. The peroxidase-like activity of the *x*Al/MIL-100(Fe) nanozymes was evaluated in the typical H_2O_2-TMB reaction system (Figure 3A).[42−45] We first determined the optimized reaction conditions with the temperature of 37 °C, pH 3.6, and the concentrations of H_2O_2 (1 mM) and TMB (0.5 mM, Figure S3). Note that MIL-100(Fe) modified by one-cycle Al_2O_3 (atomic ultrathin modification) shows the best peroxidase-like activity, while the continued increase of Al_2O_3 ALD cycles causes the activity decrease owing to the probable coverage of the MIL-100(Fe) active sites. The Al content in the 1Al/MIL-100(Fe), 3Al/MIL-100(Fe), 6Al/MIL-100(Fe), and 12Al/MIL-100(Fe) nanozymes is also determined (Figure 3B), respectively. These results demonstrate that ALD is a fine and promising approach for decorating the ultralow amount of Al_2O_3 to improve the peroxidase-like activity.

To evaluate the activity enhancement mechanism of the prepared MIL-100(Fe) and optimized 1Al/MIL-100(Fe), steady-state kinetic experiments were conducted by separately adjusting the concentration of H_2O_2 or TMB (Figures 4 and S4). The kinetic parameters were obtained by fitting the data according to the Michaelis−Menten equation, and the absorbance of reaction products catalyzed by MIL-100(Fe) and 1Al/MIL-100(Fe) nanozymes was recorded over time under specific reaction conditions. Nanozyme parameters were determined using the characteristic double reciprocal Lineweaver−Burk diagram. The K_m values (2.4×10^{-5} mM for H_2O_2 and 9.1×10^{-5} mM for TMB, Figures 4E and S4E) of 1Al/MIL-100(Fe) nanozymes were significantly lower than that of MIL-100(Fe) nanozymes (2.1×10^{-4} mM for H_2O_2 and 1.96×10^{-4} mM for TMB, Figures 4B and S4B), indicating that 1Al/MIL-100(Fe) nanozymes exhibited a stronger affinity toward the two substrates. Moreover, as another critical parameter for evaluating the catalytic rate, V_{max} values were also calculated. The V_{max} values of 1Al/MIL-100(Fe) nanozymes were 1.33×10^{-4} mMs^{-1} for H_2O_2 and 3.03×10^{-4} mMs^{-1} for TMB, which were higher than that of

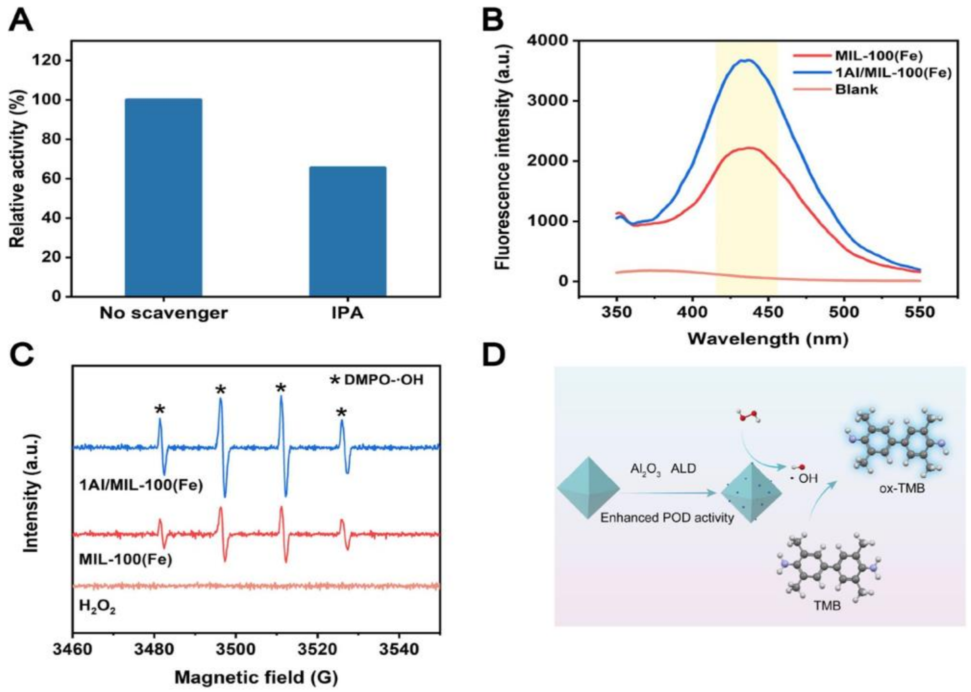

Figure 5. (A) Relative activity before and after the trapping experiments of ·OH. (B) Fluorescence spectra of blank, MIL-100(Fe), and 1Al/MIL-100(Fe). (C) ESR spectra for ·OH catalyzed by H_2O_2, MIL-100(Fe), and 1Al/MIL-100(Fe). (D) Mechanism of the reaction proposed.

MIL-100(Fe) nanozymes (6.36×10^{-5} mMs^{-1} for H_2O_2 and 2.96×10^{-4} mMs^{-1} for TMB). In addition, the two nanozymes present similar reaction orders for H_2O_2 and TMB, which indicates that the two nanozymes possess similar reaction routes and mechanisms (Figures 4C,F, and S4C,F). Therefore, 1Al/MIL-100(Fe) nanozymes possess excellent affinity and catalytic rate, leading to the excellent POD-like activity, which will be an ideal candidate for peroxidase mimics (Table S2).

3.3. Peroxidase-Like Catalytic Mechanisms of Nanozymes. ·OH is usually regarded as the active intermediate of a peroxidase-like reaction. To ascertain the ·OH generation in the reaction, ·OH trapping experiments were performed for 1Al/MIL-100(Fe) nanozymes (Figure 5A). Isopropyl alcohol (IPA) was added as the scavenger of ·OH. After adding IPA, the peroxidase-like activity of 1Al/MIL-100(Fe) is obviously inhibited, indicating that ·OH should be the major active species produced in the reaction process. To further confirm the existence of ·OH radicals, the fluorescent probe of terephthalic acid (TA) experiments was also conducted.[26] Obviously, the 1Al/MIL-100(Fe) nanozymes display a fluorescence intensity much stronger than that of pristine MIL-100(Fe) in the reactions (Figure 5B), suggesting that 1Al/MIL-100(Fe) nanozymes can promote the generation of ·OH to boost the catalytic reaction, which is in agreement with the results of the kinetic analysis above. The presence of the ·OH active species was also verified by ESR measurement. The characteristic four-line signal with a ratio of 1:2:2:1 indicates the production of ·OH radicals (Figure 5C), and the 1Al/MIL-100(Fe) nanozymes produce more ·OH than MIL-100(Fe) in the process. According to these results, the higher number of produced ·OH radicals should be responsible for the outstanding peroxidase-like activity of 1Al/MIL-100(Fe) nanozymes, and the reaction mechanism is presented in Figure 5D.

3.4. Universality of ALD Ultrathin Modification Strategy. Factually, the proposed ultrathin modification strategy of ALD is universal, and it can be used to deposit other oxides on various materials. To this end, we further deposited TiO_2 on MIL-100(Fe) by finely adjusting the ALD cycles from 0 to 12 (Figure 6A). Similarly, the 1Ti/MIL-100(Fe) nanozymes decorated with only one-cycle TiO_2 exhibit optimized POD-like activity, and excessive TiO_2 has a detrimental influence on the activity. Still, the Ti species present the atomic dispersion property (Figures 6B,C and S5). These results indicate that the decoration of an ultralow

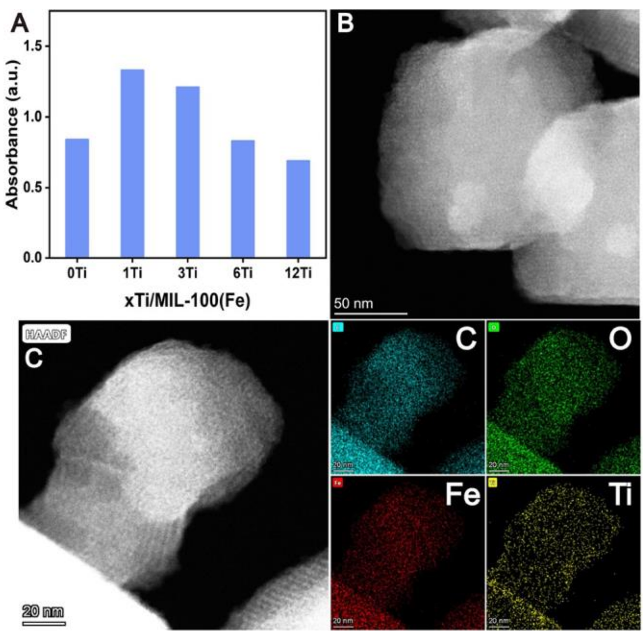

Figure 6. (A) POD-like activity comparison of the xTi/MIL-100(Fe) nanozymes. (B) HAADF-STEM and (C) corresponding EDS mapping images of 1Ti/MIL-100(Fe) nanozymes.

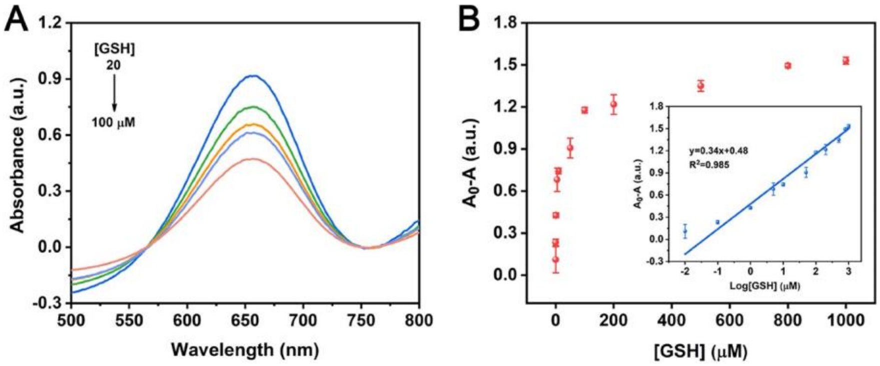

Figure 7. (A) UV−vis absorption spectra of the colorimetric system with the addition of various concentrations of GSH. (B) Plot of absorbance change ($A_0 - A$) vs GSH concentration (inset: linear calibration curves for log[GSH]).

amount of Al or Ti species can remarkably enhance the POD-like activity due to the modification of the electronic properties of the active metal.

3.5. Sensitivity and Selectivity of GSH Detection. The optimized 1Al/MIL-100(Fe) nanozyme with high stability (Figure S6) was further applied for the colorimetric analysis of GSH. As shown in Figure 7A, the absorbance of ox-TMB was progressively decreased by increasing the GSH concentration (from top to bottom: 20, 40, 60, 80, and 100 μM). It was also found that the decreased absorbance values could be linear to log[GSH] in the range of 0.01−1000 μM (Figure 7B). The LOD of the developed sensor was determined to be as low as 2.2 nM by the 3σ rule. Moreover, the 1Al/MIL-100(Fe) nanozyme-based colorimetric approach for the detection of GSH could show a broader detection range and lower LOD compared to those of previous reports (Table S3). Additionally, we have also completed the GSH detection in the fetal bovine serum (Table S4). Hence, the developed colorimetric approach should be promising for the detection of GSH in actual samples.

In addition, to evaluate the selectivity of the colorimetric system catalyzed by 1Al/MIL-100(Fe) nanozymes, the influence of different possible components (Lys, Cys, Gly, His, Cl^-, Na^+, K^+, Ca^{2+}, Thr, Arg, and Glu) that could concomitantly be present in serum was analyzed to confirm the specificity of the proposed method for GSH. Although the detection method has some response to cysteine, GSH is the most abundant biothiol in living organisms. The disturbance caused by the above species can almost be neglected although their concentration is fivefold higher than that of GSH (Figure 8), and this should be ascribed to the stronger reduction activity of GSH. These results suggest that 1Al/MIL-100(Fe) nanozymes possess excellent sensitivity and selectivity in the GSH detection reaction, and the developed colorimetric approach has a strong anti-interference ability for the detection of GSH.

These results confirm that the ultrathin-modified nanozymes have significantly enhanced POD-like activity in comparison with the as-prepared nanozymes, which should be related to Al−Fe synergy. The synthesized 1Al/MIL-100(Fe) nanozymes also show excellent sensitivity and selectivity in the GSH detection reaction. The ultrathin modification strategy of ALD could potentially be applied to the synthesis of other nanozyme systems.

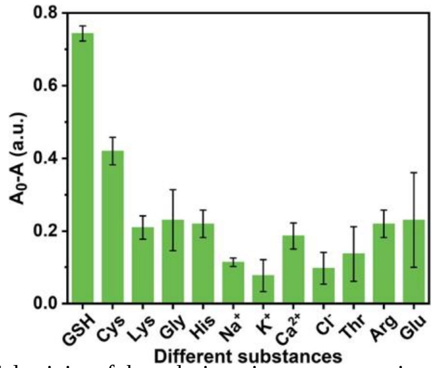

Figure 8. Selectivity of the colorimetric system to various interfering substances. The concentration of interferents is 50 μM.

4. CONCLUSIONS

In summary, the atomically dispersed 1Al/MIL-100(Fe) and 1Ti/MIL-100(Fe) nanozymes were successfully synthesized via the ultrathin modification strategy of ALD. The ultrathin modified nanozymes present much higher POD-like activity than their MIL-100(Fe) counterparts. A highly sensitive and selective colorimetric approach based on the catalysis effect was established for the quantitative detection of GSH with 1Al/MIL-100(Fe) as a high-efficiency nanozyme, which possesses high catalytic efficiency and excellent sensitivity and selectivity. Our present strategy can potentially be extended to synthesize other nanozymes with atomic dispersion for various applications.

■ ASSOCIATED CONTENT

Supporting Information

The Supporting Information is available free of charge at https://pubs.acs.org/doi/10.1021/acsanm.3c05262.

SEM, XRD, optimization of reaction temperature and pH, steady-state kinetic assays and the corresponding parameters, HAADF-STEM images, N_2 adsorption−desorption results, and detection of GSH (PDF)

■ AUTHOR INFORMATION

Corresponding Author

Jiankang Zhang − *Interdisciplinary Research Center of Biology & Catalysis, School of Life Sciences, Northwestern Polytechnical University, Xi'an 710072, P. R. China;* orcid.org/0000-0003-4483-8107; Email: zhangjiankang@nwpu.edu.cn

Authors

Lin Cui – *Interdisciplinary Research Center of Biology & Catalysis, School of Life Sciences, Northwestern Polytechnical University, Xi'an 710072, P. R. China*

Xinshuo Zhao – *Interdisciplinary Research Center of Biology & Catalysis, School of Life Sciences, Northwestern Polytechnical University, Xi'an 710072, P. R. China*

Zhan Zhou – *College of Chemistry and Chemical Engineering, Henan Key Laboratory of Function-Oriented Porous Materials, Luoyang Normal University, Luoyang 471934, P. R. China*

Dong Lin – *Max Planck-Cardiff Centre on the Fundamentals of Heterogeneous Catalysis FUNCAT, Cardiff Catalysis Institute, School of Chemistry, Cardiff University, Cardiff CF103AT, U.K.*; orcid.org/0000-0001-5313-8204

Yong Qin – *Interdisciplinary Research Center of Biology & Catalysis, School of Life Sciences, Northwestern Polytechnical University, Xi'an 710072, P. R. China; State Key Laboratory of Coal Conversion, Institute of Coal Chemistry, Chinese Academy of Sciences, Taiyuan 030001, P. R. China*; orcid.org/0000-0002-5567-1464

Complete contact information is available at:
https://pubs.acs.org/10.1021/acsanm.3c05262

Author Contributions

⊥L.C. and X.Z. contributed equally to this work.

Notes

The authors declare no competing financial interest.

ACKNOWLEDGMENTS

We appreciate the financial support from the National Natural Science Foundation of China (22372130 and 22102131) and Fundamental Research Funds for the Central Universities (G2023KY0605). We appreciate the Analytical & Testing Center of Northwestern Polytechnical University for HAADF-STEM measurements.

REFERENCES

(1) Wei, H.; Wang, E. Nanomaterials with Enzyme-like Characteristics (Nanozymes): Next-Generation Artificial Enzymes. *Chem. Soc. Rev.* 2013, *42*, 6060−6093.

(2) Liang, M.; Yan, X. Nanozymes: from New Concepts, Mechanisms, and Standards to Applications. *Acc. Chem. Res.* 2019, *52*, 2190−2200.

(3) Gao, L.; Zhuang, J.; Nie, L.; Zhang, J.; Zhang, Y.; Gu, N.; Wang, T.; Feng, J.; Yang, D.; Perrett, S.; Yan, X. Intrinsic Peroxidase-like Activity of Ferromagnetic Nanoparticles. *Nat. Nanotechnol.* 2007, *2*, 577−583.

(4) Zhang, R.; Yan, X.; Fan, K. Nanozymes Inspired by Natural Enzymes. *Acc. Mater. Res.* 2021, *2*, 534−547.

(5) Xi, J.; Wei, G.; An, L.; Xu, Z.; Xu, Z.; Fan, L.; Gao, L. Copper/Carbon Hybrid Nanozyme: Tuning Catalytic Activity by the Copper State for Antibacterial Therapy. *Nano Lett.* 2019, *19*, 7645−7654.

(6) Yang, J.; Yao, H.; Guo, Y.; Yang, B.; Shi, J. Enhancing Tumor Catalytic Therapy by Co-Catalysis. *Angew. Chem., Int. Ed.* 2022, *134*, No. e202200480.

(7) Sheng, J.; Wu, Y.; Ding, H.; Feng, K.; Shen, Y.; Zhang, Y.; Gu, N. Multienzyme-Like Nanozymes: Regulation, Rational Design, and Application. *Adv. Mater.* 2023, No. 2211210.

(8) Jiao, L.; Yan, H.; Wu, Y.; Gu, W.; Zhu, C.; Du, D.; Lin, Y. When Nanozymes Meet Single-Atom Catalysis. *Angew. Chem., Int. Ed.* 2020, *132*, 2585−2596.

(9) Zandieh, M.; Liu, J. Surface Science of Nanozymes and Defining a Nanozyme Unit. *Langmuir* 2022, *38*, 3617−3622.

(10) Fu, W.; Zhang, X.; Mei, L.; Zhou, R.; Yin, W.; Wang, Q.; Gu, Z.; Zhao, Y. Stimuli-Responsive Small-on-Large Nanoradiosensitizer for Enhanced Tumor Penetration and Radiotherapy Sensitization. *ACS Nano* 2020, *14*, 10001−10017.

(11) Yan, R.; Sun, S.; Yang, J.; Long, W.; Wang, J.; Mu, X.; Li, Q.; Hao, W.; Zhang, S.; Liu, H.; Gao, Y.; Ouyang, L.; Chen, J.; Liu, S.; Zhang, X.; Ming, D. Nanozyme-Based Bandage with Single-Atom Catalysis for Brain Trauma. *ACS Nano* 2019, *13*, 11552−11560.

(12) Ding, S.; Lyu, Z.; Fang, L.; Li, T.; Zhu, W.; Li, S.; Li, X.; Li, J.; Du, D.; Lin, Y. Single-Atomic Site Catalyst with Heme Enzymes-Like Active Sites for Electrochemical Sensing of Hydrogen Peroxide. *Small* 2021, *17*, No. 2100664.

(13) Yang, H.; Xu, B.; Li, S.; Wu, Q.; Lu, M.; Han, A.; Liu, H. A Photoresponsive Nanozyme for Synergistic Catalytic Therapy and Dual Phototherapy. *Small* 2021, *17*, No. 2007090.

(14) Wu, J.; Wang, X.; Wang, Q.; Lou, Z.; Li, S.; Zhu, Y.; Qin, L.; Wei, H. Nanomaterials with Enzyme-like Characteristics (Nanozymes): Next-Generation Artificial Enzymes (II). *Chem. Soc. Rev.* 2019, *48*, 1004−1076.

(15) Korschelt, K.; Tahir, M. N.; Tremel, W. A Step into the Future: Applications of Nanoparticle Enzyme Mimics. *Chem.—Eur. J.* 2018, *24*, 9703−9713.

(16) Mao, Y. W.; Zhang, J.; Zhang, R.; Li, J. Q.; Wang, A. J.; Zhou, X. C.; Feng, J. J. N-Doped Carbon Nanotubes Supported Fe−Mn Dual-Single-Atoms Nanozyme with Synergistically Enhanced Peroxidase Activity for Sensitive Colorimetric Detection of Acetylcholinesterase and Its Inhibitor. *Anal. Chem.* 2023, *95*, 8640−8648.

(17) Jiang, B.; Duan, D.; Gao, L.; Zhou, M.; Fan, K.; Tang, Y.; Xi, J.; Bi, Y.; Tong, Z.; Gao, G. F.; Xie, N.; Tang, A.; Nie, G.; Liang, M.; Yan, X. Standardized Assays for Determining the Catalytic Activity and Kinetics of Peroxidase-like Nanozymes. *Nat. Protoc.* 2018, *13*, 1506−1520.

(18) Liu, B.; Liu, J. Surface Modification of Nanozymes. *Nano Res.* 2017, *10*, 1125−1148.

(19) Cheng, H.; Zhang, L.; He, J.; Guo, W.; Zhou, Z.; Zhang, X.; Nie, S.; Wei, H. Integrated Nanozymes with Nanoscale Proximity for in Vivo Neurochemical Monitoring in Living Brains. *Anal. Chem.* 2016, *88*, 5489−5497.

(20) Wei, H.; Wang, E. Fe_3O_4 Magnetic Nanoparticles as Peroxidase Mimetics and Their Applications in H_2O_2 and Glucose Detection. *Anal. Chem.* 2008, *80*, 2250−2254.

(21) Lin, Y.; Ren, J.; Qu, X. Catalytically Active Nanomaterials: A Promising Candidate for Artificial Enzymes. *Acc. Chem. Res.* 2014, *47*, 1097−1105.

(22) Li, B.; Chu, D.; Cui, H.; Li, Z.; Zhou, Z.; Tan, C.; Li, J. Activating MoO_3 Nanobelts via Aqueous Intercalation as a Near Infrared Type I Photosensitizer for Photodynamic Periodontitis Treatment. *SmartMat* 2023, *4*, No. e1243, DOI: 10.1002/smm2.1243.

(23) Zhou, Z.; Wang, T.; Hu, T.; Cheng, C.; Yu, S.; Li, H.; Liu, S.; Ma, L.; Zhao, M.; Liang, R. Facile Synthesis of 2D Al-TCPP MOF Nanosheets for Efficient Sonodynamic Cancer Therapy. *Mater. Chem. Front.* 2023, *7*, 1684−1693.

(24) Xue, B.; Geng, X.; Cui, H.; Chen, H.; Wu, Z.; Chen, H.; Li, H.; Zhou, Z.; Zhao, M.; Tan, C.; Li, J. Size Engineering of 2D MOF Nanosheets for Enhanced Photodynamic Antimicrobial Therapy. *Chin. Chem. Lett.* 2023, *34*, No. 108140.

(25) Zhao, X.; Qiu, H.; Shao, Y.; Wang, P.; Yu, S.; Li, H.; Zhou, Y.; Zhou, Z.; Ma, L.; Tan, C. Silver Nanoparticle-Modified 2D MOF Nanosheets for Photothermally Enhanced Silver Ion Release Antibacterial Treatment. *Acta Phys. Chim. Sin.* 2023, *39*, No. 2211043.

(26) Qin, F.; Zhang, J.; Zhou, Z.; Xu, H.; Cui, L.; Lv, Z.; Qin, Y. TiO_2 Nanoflowers Decorated with FeO_x Nanocluster and Single Atoms by Atomic Layer Deposition for Peroxidase-Mimicking Nanozymes. *ACS Appl. Nano Mater.* 2022, *5*, 13090−13099.

(27) Jia, L.; Niu, L. Y.; Yang, Q. Z. Fluorescent Probe for Simultaneous Discrimination of GSH, Cys, and SO_2 Derivatives. *Anal. Chem.* 2020, *92*, 10800−10806.

(28) Umezawa, K.; Yoshida, M.; Kamiya, M.; Yamasoba, T.; Urano, Y. Rational Design of Reversible Fluorescent Probes for Live-Cell Imaging and Quantification of Fast Glutathione Dynamics. *Nat. Chem.* 2017, *9*, 279−286.
(29) Ji, X.; Lu, Q.; Sun, X.; Zhao, L.; Zhang, Y.; Yao, J.; Zhang, X.; Zhao, H. Dual-Active Au@PNIPAm Nanozymes for Glucose Detection and Intracellular H_2O_2 Modulation. *Langmuir* 2022, *38*, 8077−8086.
(30) Wang, X.; Qin, L.; Lin, M.; Xing, H.; Wei, H. Fluorescent Graphitic Carbon Nitride-Based Nanozymes with Peroxidase-Like Activities for Ratiometric Biosensing. *Anal. Chem.* 2019, *91*, 10648−10656.
(31) Peng, D.; Yang, Y.; Que, M.; Ding, Y.; Wu, M.; Deng, X.; He, Q.; Ma, X.; Li, X.; Qiu, H. Partially Oxidized MoS_2 Nanosheets with High Water-Solubility to Enhance the Peroxidase-Mimic Activity for Sensitive Detection of Glutathione. *Anal. Chim. Acta* 2023, *1250*, No. 340968.
(32) Tadepalli, S.; Wang, Z.; Liu, K. K.; Jiang, Q.; Slocik, J.; Naik, R. R.; Singamaneni, S. Influence of Surface Charge of the Nanostructures on the Biocatalytic Activity. *Langmuir* 2017, *33*, 6611−6619.
(33) Zhang, J.; Yang, Y.; Qin, F.; Hu, T.; Zhao, X.; Zhao, S.; Cao, Y.; Gao, Z.; Zhou, Z.; Liang, R.; Tan, C.; Qin, Y. Catalyzing Generation and Stabilization of Oxygen Vacancies on CeO_{2-x} Nanorods by Pt Nanoclusters as Nanozymes for Catalytic Therapy. *Adv. Healthc. Mater.* 2023, *12*, No. 2302056.
(34) Zhang, J.; Pan, Y.; Feng, D.; Cui, L.; Zhao, S.; Hu, J.; Wang, S.; Qin, Y. Mechanistic Insight into the Synergy between Platinum Single Atom and Cluster Dual Active Sites Boosting Photocatalytic Hydrogen Evolution. *Adv. Mater.* 2023, *35*, No. 2300902.
(35) Zhang, J.; Yu, W.; Feng, D.; Xu, H.; Qin, Y. Porous Titania Nanotube Confined Ultrafine Platinum Catalysts Synthesized by Atomic Layer Deposition with Enhanced Hydrolytic Dehydrogenation Performance. *Appl. Catal. B Environ.* 2022, *312*, No. 121405.
(36) Zhang, J.; Yu, Z.; Gao, Z.; Ge, H.; Zhao, S.; Chen, C.; Chen, S.; Tong, X.; Wang, M.; Zheng, Z.; Qin, Y. Porous TiO_2 Nanotubes with Spatially Separated Platinum and CoO_x Cocatalysts Produced by Atomic Layer Deposition for Photocatalytic Hydrogen Production. *Angew. Chem., Int. Ed. Engl.* 2017, *56*, 816−820.
(37) Zhang, J.; Chen, C.; Yan, W.; Duan, F.; Zhang, B.; Gao, Z.; Qin, Y. Ni Nanoparticles Supported on CNTs with Excellent Activity Produced by Atomic Layer Deposition for Hydrogen Generation from the Hydrolysis of Ammonia Borane. *Catal. Sci. Technol.* 2016, *6*, 2112−2119.
(38) Zhang, J.; Zheng, X.; Yu, W.; Feng, X.; Qin, Y. Unravelling the Synergy in Platinum-Nickel Bimetal Catalysts Designed by Atomic Layer Deposition for Efficient Hydrolytic Dehydrogenation of Ammonia Borane. *Appl. Catal. B Environ.* 2022, *306*, No. 121116.
(39) Zhang, J.; Gao, Z.; Wang, S.; Wang, G.; Gao, X.; Zhang, B.; Xing, S.; Zhao, S.; Qin, Y. Origin of Synergistic Effects in Bicomponent Cobalt Oxide-Platinum Catalysts for Selective Hydrogenation Reaction. *Nat. Commun.* 2019, *10*, 4166.
(40) Jin, Y.; Mi, X.; Qian, J.; Ma, N.; Dai, W. Modular Construction of an MIL-101(Fe)@MIL-100(Fe) Dual-Compartment Nanoreactor and Its Boosted Photocatalytic Activity toward Tetracycline. *ACS Appl. Mater. Interfaces* 2022, *14*, 48285−48295.
(41) Lupu, D.; Ardelean, O.; Blanita, G.; Borodi, G.; Lazar, M. D.; Biris, A. R.; Ioan, C.; Mihet, M.; Misan, I.; Popeneciu, G. Synthesis and Hydrogen Adsorption Properties of a New Iron Based Porous Metal-Organic Framework. *Int. J. Hydrogen Energy* 2011, *36*, 3586−3592.
(42) Jiang, B.; Duan, D.; Gao, L.; Zhou, M.; Fan, K.; Tang, Y.; Xi, J.; Bi, Y.; Tong, Z.; Gao, G.; Xie, N.; Tang, A.; Nie, G.; Liang, M.; Yan, X. Standardized Assays for Determining the Catalytic Activity and Kinetics of Peroxidase-Like Nanozymes. *Nat. Protoc.* 2018, *13*, 1506−1520.
(43) Dong, H.; Du, W.; Dong, J.; Che, R.; Kong, F.; Cheng, W.; Ma, M.; Gu, N.; Zhang, Y. Depletable Peroxidase-Like Activity of Fe_3O_4 Nanozymes Accompanied with Separate Migration of Electrons and Iron Ions. *Nat. Commun.* 2022, *13*, 5365.
(44) Nguyen, P.; Lee, J.; Cho, A.; Kim, M.; Choi, D.; Han, J.; Kim, M.; Lee, J. Rational Development of Co-Doped Mesoporous Ceria with High Peroxidase-Mimicking Activity at Neutral pH for Paper-Based Colorimetric Detection of Multiple Biomarkers. *Adv. Funct. Mater.* 2022, *32*, No. 2112428.
(45) Zhu, C.; Zhou, Z.; Gao, X.; Tao, Y.; Cao, X.; Xu, Y.; Shen, Y.; Liu, S.; Zhang, Y. Cascade Nanozymatic Network Mimicking Cells with Selective and Linear Perception of H_2O_2. *Chem. Sci.* 2023, *14*, 6780−6791.